Journal of Molecular Catalysis A: Chemical 423 (2016) 441–448

Contents lists available at ScienceDirect

Journal of Molecular Catalysis A: Chemical

journal homepage: www.elsevier.com/locate/molcata

Maleic anhydride hydrogenation to succinic anhydride over mesoporous Ni/TiO_2 catalysts: Effects of Ni loading and temperature

Cecilia C. Torres[a,*], Joel B. Alderete[a], Claudio Mella[b], Barbara Pawelec[c]

[a] Departamento de Química Orgánica, Universidad de Concepción, Edmundo Larenas 129, Concepción, Chile
[b] Departamento de Fisicoquímica, Universidad de Concepción, Edmundo Larenas 129, Concepción, Chile
[c] Instituto de Catálisis y Petroleoquímica (ICP-CSIC), Sustainable Energy and Chemistry Group, Marie Curie 2 Cantoblanco Madrid, Spain

ARTICLE INFO

Article history:
Received 4 June 2016
Received in revised form 19 July 2016
Accepted 20 July 2016
Available online 21 July 2016

Keywords:
Maleic anhydride
Nickel
Hydrogenation
Recycle
Succinic anhydride

ABSTRACT

Catalytic hydrogenation of maleic anhydride for the production of succinic anhydride can be a viable alternative to the higher energetic demand route based in the dehydration of succinic acid. In this sense, the metallic Ni catalysts supported on mesoporous TiO_2 (anatase) substrate demonstrated to be very active and 100% selective in the liquid phase hydrogenation of maleic anhydride (MA) to succinic anhydride (SA). The catalysts, which were prepared via wet impregnation method with different Ni loading (5, 10 and 15 wt.%), were characterized by chemical analysis (ICP-AES), N_2 physical adsorption- desorption, H_2- temperature programmed reduction (H_2- TPR), X-ray diffraction (XRD), high resolution transmission electron spectroscopy (HR-TEM) and X-ray photoelectron spectroscopy (XPS). The Ni species interaction with support was investigated by TPR and by performing five catalyst recycling tests. After catalyst activation by reduction, the increase of Ni particle size with an increase of Ni loading was relatively small (from 6.9 to 8.9 nm) due to enhance of the metal-support interaction. After the first catalytic cycle, the optimized 5%Ni/TiO_2 catalyst showed a small decrease in the Ni loading attributed to metal leaching during time course of reaction. Besides this, the 5%Ni/TiO_2 catalyst exhibited a good stability during five continuous cycles with a very high yield of SA after 5 cycles. Finally, temperature experiments performed for the best system shown that the reaction temperature does not affect the SA selectivity in the temperature range studied (323 K–398 K).

1. Introduction

For years the chemical industry has search efficient methods to optimize yield and selectivity of reactions that are part of different types of processes used for the production of intermediate products, which are used in diverse applications. This wide range of products include those obtained in the fine chemical industry, for which usually both yield and selectivity can be achieved using catalysts operating in heterogeneous phase [1,2]. Among building blocks molecules, maleic anhydride is highlighted, which is produced on a large scale by the partial oxidation of n-butane [3,4]. The catalytic hydrogenation of MA both in liquid phase and gas phase [5–8], give products such as succinic anhydride (SA), γ-butyrolactone (GBL), tetrahydrofuran (THF), among others (see Scheme 1). In particular, SA is used as raw material in the production of a wide variety of substances, which are used as colorants, fragrances, flavorings, etc. [9]. The obtention of SA at large scale is performed by the dehydration of succinic acid, which proceeds at elevated temperatures (523 K). However, obtaining SA from the catalytic hydrogenation of MA represents an alternative route to its traditional production, since the use of catalysts operating at lower temperature should decrease the energy requirements of the process compared with the route of dehydration of the succinic acid [10].

In general, the hydrogenation of MA has been studied using different types of catalysts, as it is summarized in Table 1.

Noble metals, transition metals with hydrogenating activity and combinations of both have shown to be active in the hydrogenation reaction of MA and selectivity dependence to SA was observed, mainly due to the nature of the support and the active phase used. Moreover, most of these catalytic systems are characterized by operating at temperatures above 453 K, and at high hydrogen pressure (5.0 MPa or higher). Of the active phases studied, nickel has proven to be a good alternative due to the high affinity that this metal has for the activation of C—C double bonds (seen Table 1). However, the ability of nickel to produce hydrogenoly-

* Corresponding author.
E-mail address: cectorres@udec.cl (C.C. Torres).

http://dx.doi.org/10.1016/j.molcata.2016.07.037
1381-1169/

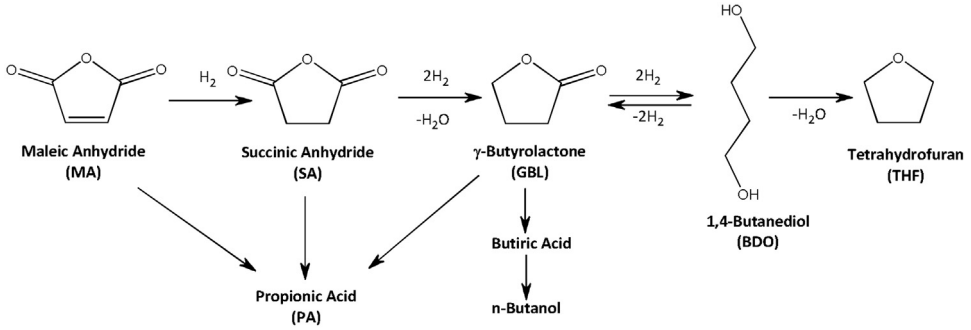

Scheme 1. Reaction pathway of the hydrogenation of maleic anhydride adapted from [11].

Table 1
Comparison of the selectivity toward succinic anhydride in liquid-phase hydrogenation of maleic anhydride over different supported catalysts.

Catalyst	Conditions	S_{SA} (%)	Reference
2%Ru/AC	T = 423 K; P_{H2} = 6.0 MPa; 2.0 mol L^{-1} MA; 0.050 g catalyst	99.6 (2)[a]	[11]
8%Pd-4%Zr/SiO_2	T = 513 K; P_{H2} = 7.1 MPa; 3.1 mol L^{-1} MA;10.0 g catalyst	51.5 (4)[a]	[12]
3%Ru-25%Ni/SiO_2	T = 513 K; P_{H2} = 7.1 MPa; 3.1 mol L^{-1} MA; 10 g catalyst	73.2 (5)[a]	[12]
10%Ni/CeO_2	T = 483 K; P_{H2} = 5.0 MPa; 1.25 mol L^{-1} MA; 0.10 g catalyst	65.0 (8)[a]	[13]
10%Ni/Al_2O_3	T = 483 K; P_{H2} = 5.0 MPa; 1.25 mol L^{-1} MA; 0.10 g catalyst	85.0 (8)[a]	[13]

[a] Total reaction time in hours.

sis of C=O bonds [14–16] could significantly reduce the selectivity towards SA. In relation to the support, it plays a fundamental role in the performance of the catalytic hydrogenation of MA. Thus, supported catalysts on partially reducible oxides, such as TiO_2 or CeO_2, able to generate *strong metal support interaction* (SMSI), have shown a decreasing selectivity toward SA, favoring the production of GBL. This is due to the strong support-carbonyl bonds interactions [6,12,17,18]. Therefore, an efficient and selective catalyst to SA, possessing Ni as active phase, should employ supports in which strong metal-support interactions are not established or they are strongly diminished.

Among different supports, the new synthesized mesoporous TiO_2 of pure anatase phase demonstrated to be a good substrate for supporting metal oxides due to the strong metal support interaction (SMSI), chemical stability, acid-base property, sharp pore distribution and large surface favoring good active phase dispersion [19,20]. The active phase dispersion could be enhanced also by using optimized catalyst's preparation conditions. In this context, the study by Huo et al. [18] demonstrated that calcination temperature strongly influenced on the catalytic behavior of Ni/TiO_2 catalysts tested in hydrogenation of MA. This is probably because of the morphological changes occurring upon high temperature calcination influencing on the metal-TiO_2 support interaction, such as sintering [21], encapsulation or interdiffusion [22]. Thus, the temperature of calcination should be carefully selected in order to decompose Ni precursor without producing those undesirable phenomena.

Within this scenario, the present work was undertaken with the aim to evaluate the catalytic response of Ni catalysts supported on TiO_2 (anatase) substrate for hydrogenation of maleic anhydride (MA) to succinic anhydride (SA). In addition, the recycling tests have been performed in order to evaluate the stability of Ni species on the support surface during liquid phase reaction. For the best catalyst (5%Ni/TiO_2), the effect of reaction temperature on the catalyst activity was also investigated. In order to explain the catalytic behavior, the nature of nickel species for different Ni loadings (5, 10 and 15 wt.%) and their interaction with the support have been investigated by means of different characterization techniques (XRD, TPR, HR-TEM and XPS).

2. Experimental

2.1. Catalyst preparation

All catalytic systems were prepared by the wet impregnation procedure using a slight excess of deionized water [23]. The proper amount of metallic precursor, $Ni(NO_3)_2 \times 6H_2O$, was added to 5.0 g of TiO_2-anatase in order to obtain 5, 10 and 15% wt. of nickel, subsequently 50 mL of deionized water was incorporated. This procedure was performed in a rotary evaporator at 343 K for 5 h [24]. The resulting solid was filtered until the filtered water showed constant conductivity. Finally, the solids were dried in an oven at 373 K overnight. The solids were calcined under air flow at 773 K for 2 h and then reduced *in situ* at 723 K under H_2 flow for 4 h [25].

2.2. Characterization

The interaction of hydrogen with the Ni catalysts was studied by temperature-programmed reduction experiments (TPR), the catalysts were reduced under continuous flow using a 5% H_2/Ar mixture (40 cm^3 min^{-1}), at 10 K min^{-1} from room temperature up to 1073 K in a TPR/TPD2900 Micromeritics system. Hydrogen consumption was monitored with the aid of a TCD detector and recorded for TPR analysis.

X-ray diffraction (XRD) was performed on a Rigaku X-ray Geigerflex using a Ni filter and Cu Kα radiation at 2–90° in 2θ range. N_2 adsorption-desorption isotherms were recorded at 77 K in an ASAP 2010 Micromeritics apparatus, the specific surface areas were determined by the BET (Brunauer-Emmett-Teller) equation using the adsorption data over a relative pressure range of 0.05–0.3, and the pore-size distributions were estimated using the Barrett–Joyner–Halenda (BJH) method based on the Kelvin equation [26].

A JEM-2100F Field Emission Electron Microscope (HR-TEM) featuring ultrahigh resolution and rapid data acquisition with a probe size under 0.5 nm was used to analyze the catalysts. The samples for analysis were prepared by dispersion in ethanol/H_2O (1:1) and deposited on a holey carbon/Cu grid (300 mesh). Up to 300 individual metal particles were counted for each catalyst, and the surface

area-weighted mean diameter (d_p) was calculated by the equation:

$$d_p = \frac{\sum_i n_i d_i^3}{\sum_i n_i d_i^2}$$

where n_i is the number of particles of diameter d_i.

Chemical analysis was performed by inductively coupled plasma-mass spectrometry on a PerkinElmer 3300 ICP-MS Spectrometer. Samples were solubilized in a nitric/hydrochloric acid solution and homogenized in microwave oven.

X-ray photoelectron spectra (XPS) of the *in-situ* reduced (723 K for 2 h) catalysts were recorded using an Escalab 200R spectrometer provided with a hemispherical analyzer, operated in a constant pass energy mode and Mg Kα X-ray radiation (h = 1253.6 eV) operated at 10 mA and 12 kV. Charging effects of samples were corrected by fixing the binding energy (BE) of the C1s core-level of adventitious carbon at 284.8 eV (accuracy = ± 0.1 eV).

2.3. Catalytic activity in liquid phase

The catalytic assays of maleic anhydride hydrogenation were performed in a stainless steel (150 mL) Parr-type semi-batch reactor using a substrate/metal ratio of 100, stirring rate of 650 rpm, 50 mL of tetrahydrofuran (THF) as the solvent and 0.100 g of catalyst. Before reaction, the *x*%Ni/TiO_2 catalysts were activated by reduction with H_2 at 723 K for 2 h. Maleic anhydride hydrogenation kinetic experiments were carried out between 323 and 393 K and a total hydrogen pressure of 4.0 MPa. No mass transfer resistance were found in a catalytic test established using the Madon and Boudart approach [27]. No catalytic activity for pure TiO_2 was confirmed in a blank test. Pseudo-first-order kinetic constants (k) were calculated as reported in previous studies [28]. Analytical quantifications for reactants and products were analyzed by gas chromatography using a GC instrument, HP-4890 with a semi-capillary column HP-5, FID detector and N_2 as the carrier gas. Temperature and reusability studies were performed with the best catalytic system. The recycling assays were performed by centrifugation of the catalyst from the reaction medium, washed four times consecutively with ethanol (40 mL × 4) to clean the surface and removed all organic matter, dried under vacuum at 323 K for 12 h and finally reduced at 473 K for 1 h under H_2 flow [29].

2.4. Ni-leaching tests

The screening catalytic assays of residual filtered catalytic reaction was studied in the cyclohexene hydrogenation and performed in a stainless steel (150 mL) Parr-type semi-batch reactor at a substrate/metal ratio of 250, assumed from ICP-AES post-reaction characterization, at 650 rpm under 4.0 MPa of H_2 pressure and 373 K of temperature and reaction time of 4 h.

3. Results and discussion

3.1. Catalysts characterization

Fig. 1 presents XRD profiles of the TiO_2-anatase and Ni catalysts. In all of the patterns the diffraction planes associated at 2θ angles of 25.4°, 37.9° and 48.2° of typical TiO_2-anatase were observed (JCPDS 00-021-1272) [30–32]. These diffraction peaks were unchanged after deposition of the metal phase. In all three catalysts signals at 2θ angles of 44.5° and 52.0° are observed, which are associated with diffraction planes (111) and (200) of the metallic nickel (Ni^0) [33,34]. In addition, an increase in the intensity of the diffraction peak associated to Ni^0 (2θ = 44.5°) was observed with the increase of nominal metal loading. The observed increase in the signal intensity might indicate an increase in the crystallinity of metallic Ni particles whereas the decrease in their average crystallite size could be deduced from an increase of the full width at half maximum of the peaks. For all catalysts, no peaks due to crystalline Ni_xO_y-type species were observed. This observation suggests that their crystal size could be below detection limit of XRD technique (<4 nm) indicating the high Ni species dispersion on the support surface [18] and/or because they are not crystalline (amorphous).

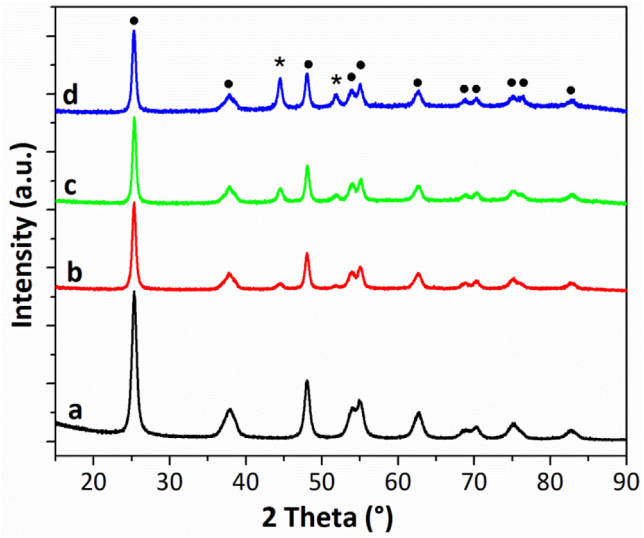

Fig. 1. Diffraction patterns for (a) TiO_2, (b) 5%Ni/TiO_2, (c) 10%Ni/TiO_2 and (d) 15%Ni/TiO_2. Reference patterns (*) Ni^0 (JCPDS 00-004-0850); (●) TiO_2-Anatase (JCPDS 00-021-1272).

Table 2
Structural and morphological analysis of TiO_2-anatase support and Ni-TiO_2 supported catalysts.

Sample	S_{BET}[a] ($m^2\ g^{-1}$)	d_p (nm)[b]	V_p[c] ($cm^3\ g^{-1}$)
TiO_2	156	8.5	0.37
5%Ni/TiO_2	107	9.7	0.30
10%Ni/TiO_2	92	10.3	0.27
15%Ni/TiO_2	87	9.7	0.23

[a] Specific surface area, determined by the BET method from N_2 physisorption measurements.
[b] Pore diameter, determined from quantity of N_2 adsorbed at a relative pressure = 0.99.
[c] Pore volume, calculated from the maximum in the BJH pore size distribution.

The textural and morphological properties of the different systems were analyzed by N_2 desorption- adsorption isotherms at 77 K. As shown in Fig. 2, all the systems give type IV isotherms according to the IUPAC classification, corresponding to mesoporous materials with cylindrical pores [35]. In addition, it can be observed that the pore distribution is bimodal for all systems, centered at 7.0 and 11.0 nm approximately. This distribution is due to interparticle porosity which is characteristic of TiO_2 based supports [36]. Table 2 shows the values associated with the textural properties of the support and catalysts. As shown in Table 2 no significant variations in the surface area, diameter, and pore volume were observed, when the values associated to the support and catalysts were compared. This could indicate that the morphological properties of the material remain unchanged after the incorporation of metal despite the small pore blockage, which is reflected in the small decrease of the surface area of the catalysts.

The morphology of the pure TiO_2 substrate and *x*%Ni/TiO_2 catalysts was examined by HRTEM. HR-TEM images of *x*%Ni/TiO_2 catalysts together with that of pure TiO_2 anatase support are shown in Fig. 3.

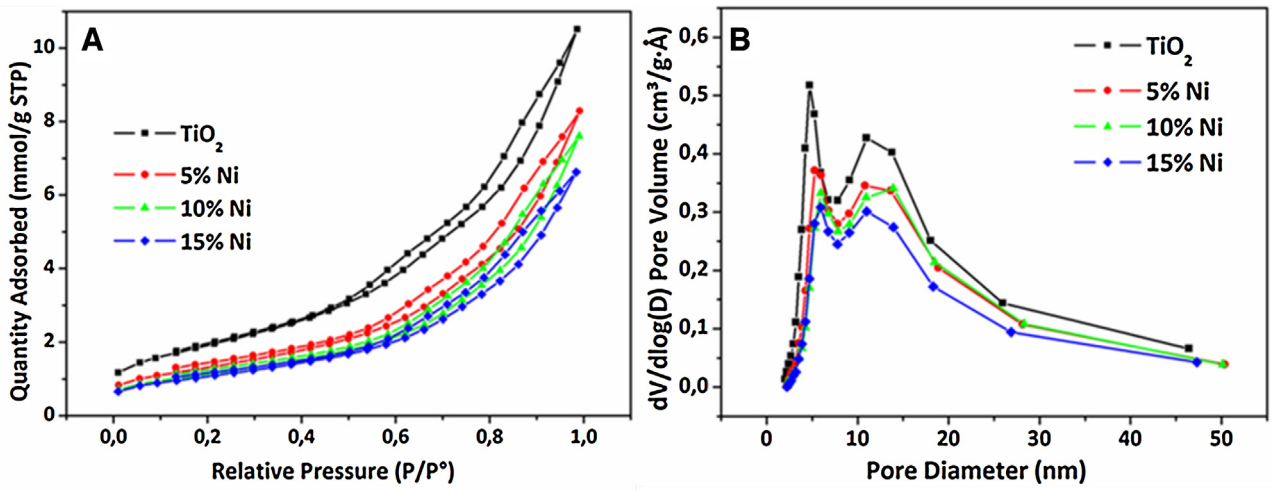

Fig. 2. N_2 adsorption-desorption isotherms at 77 K (A) and pore size distributions (B) of the support and their respective catalysts.

Table 3
ICP-AES and metal particle size distribution determined by TEM for Ni/TiO_2 catalysts.

Sample	Ni wt. (%)[a]	d_{XRD} (nm)[b]	$d_{HR\text{-}TEM}$ (nm)[c]	D_{TEM}(%)[d]
5%Ni/TiO_2	4.5 (4.0)[a]	8.0	6.9 ± 0.8	15.0
10%Ni/TiO_2	9.1 (4.4)[a]	9.0	8.0 ± 1.1	13.0
15%Ni/TiO_2	14.6 (5.7)[a]	11.9	8.9 ± 1.2	11.3

[a] Nickel loading of the fresh reduced samples before and after reaction (in parenthesis).
[b] Ni^0 particle size (from XRD) calculated using equation $d = \frac{0.94\lambda}{\beta_{1/2}\cos\theta}$.
[c] Particle size determinated by statistical analysis of different HR-TEM images.
[d] Catalyst dispersion (from HR-TEM) calculated using equation $D = \frac{1.01}{d_{HR-TEM}} \times 100\%$ [37].

Table 4
Binding energies (eV) of internal electrons and Ni/Ti atomic surface ratio of *x*%Ni/TiO_2 systems after *in-situ* H_2-reduction at 723 K for 2 h.

Catalyst	$Ti2p_{3/2}$	O1s	$Ni2p_{3/2}$[a]	Ni/Ti at
5%Ni/TiO_2	458.6	529.9 (83) 531.5 (17)	852.4 (61) 855.4 (39)	0.050
10%Ni/TiO_2	458.6	530.1 (81) 531.6 (19)	852.2 (64) 855.4 (36)	0.096
15%Ni/TiO_2	458.6	529.9 (85) 531.5 (15)	852.2 (67) 855.3 (33)	0.144

[a] The percentage of the corresponding species are given in parenthesis.

According to the EDX information, the black dots seen on the support matrix of *x*%Ni/TiO_2 catalysts are assumed to be metallic Ni particles. All *x*%Ni/TiO_2 catalysts exhibit the structure of titanium oxide decorated with metallic Ni particles. The metal particles have almost regular spherical shapes in all catalytic systems. The influence of Ni loading on the Ni particle size distributions could be deduced from the histograms of the 5%Ni/TiO_2, 10%Ni/TiO_2 and 15%Ni/TiO_2 catalysts shown in Fig. 3 together with the corresponding TEM images. The average particle diameter determined by statistical analysis is listed in Table 3. As seen, the average Ni particle size follows the trend: 5%Ni/TiO_2 (6.9 ± 0.8 nm) < 10%Ni/TiO_2 (8.0 ± 1.1 nm) < 15%Ni/TiO_2 (8.9 ± 1.2 nm). As expected, when the nickel content increases the size of the metallic crystals also slightly increased. This result is according with the results observed in XRD. As a general trend, a more heterogeneous distribution of Ni agglomerates can be observed for the catalysts with higher Ni loading (10 and 15 wt.%) than for the sample with a low Ni loading (5%Ni/TiO_2).

Through ICP-AES analysis the amount of metal in the catalysts was determined. This analysis revealed that the actual amount of metal is very close to the nominal amount, showing that the preparation method does not present significant loss of metal in both the impregnation step and subsequent reduction of the catalysts (see Table 3).

The catalysts were prepared by impregnation of TiO_2 substrate with the nickel precursor followed by drying and calcination at 773 K in dynamic air flow. Under these conditions, the formation of nickel species, such as Ni_xO_y and $NiTiO_3$ is precluded. These oxidic species are undesired because Ni^0 is the active species in the hydrogenation reaction. It is also emphasized that if "NiO(core)-$NiTiO_3$(shell)" structures are formed, then the reducibility of nickel oxide species could be strongly affected, as it was observed by Hou et al. [18].

Temperature-programmed reduction (TPR) studies of TiO_2-supported nickel oxide have been used to evaluate the influence of nickel oxide loading on the metal-support interaction. In Fig. 4 the TPR-H_2 profiles for the systems synthesized are shown. In all the catalysts, metal reduction in two or more steps was observed. The first one is a reduction peak of equal intensity for the three metal content, centered at 553 K, which may be associated with Ni_xO_y species that interact weakly with the support (TiO_2-anatase) [38]. For 5%Ni/TiO_2 catalyst, a second reduction peak is observed at 620 K attributed to the reduction of Ni_xO_y species interacting more strongly with the support. For 10%Ni/TiO_2 and 15%Ni/TiO_2 catalysts, this peak is shifted toward higher reduction temperature (649 K), thus, the interaction of those species with support could be stronger. Noticeably, the latter peak exhibits small shoulder at lower temperature region, which could be attributed to the reduction of Ni_xO_y species having intermediate size [18,34,39].

X-ray spectrophotometry analysis (XPS) was performed to the samples pre-reduced at the same conditions as those used for reaction tests. Using this technique the surface composition and electronic states of the different elements in the catalysts were determined. Ni 2p spectrum (not shown here) shows two contributions, as summarized in Table 4, indicating that *in-situ* H_2-reduction at 723 K for 2 h is not strong enough to reduce completely Ni^{2+},ions, in good agreement with TPR characterization (Fig. 4). These signals indicate the presence of Ni^0 (BE at 852.4 ± 0.2 eV) and Ni^{2+} (BE at 855.4 ± 0.2 eV) species [40,41]. The contribution of Ni^{2+} in the catalysts can be explained by the presence of highly disperse surface Ni_xO_y species, which possesses small sizes as can be inferred from the characterization by XRD.

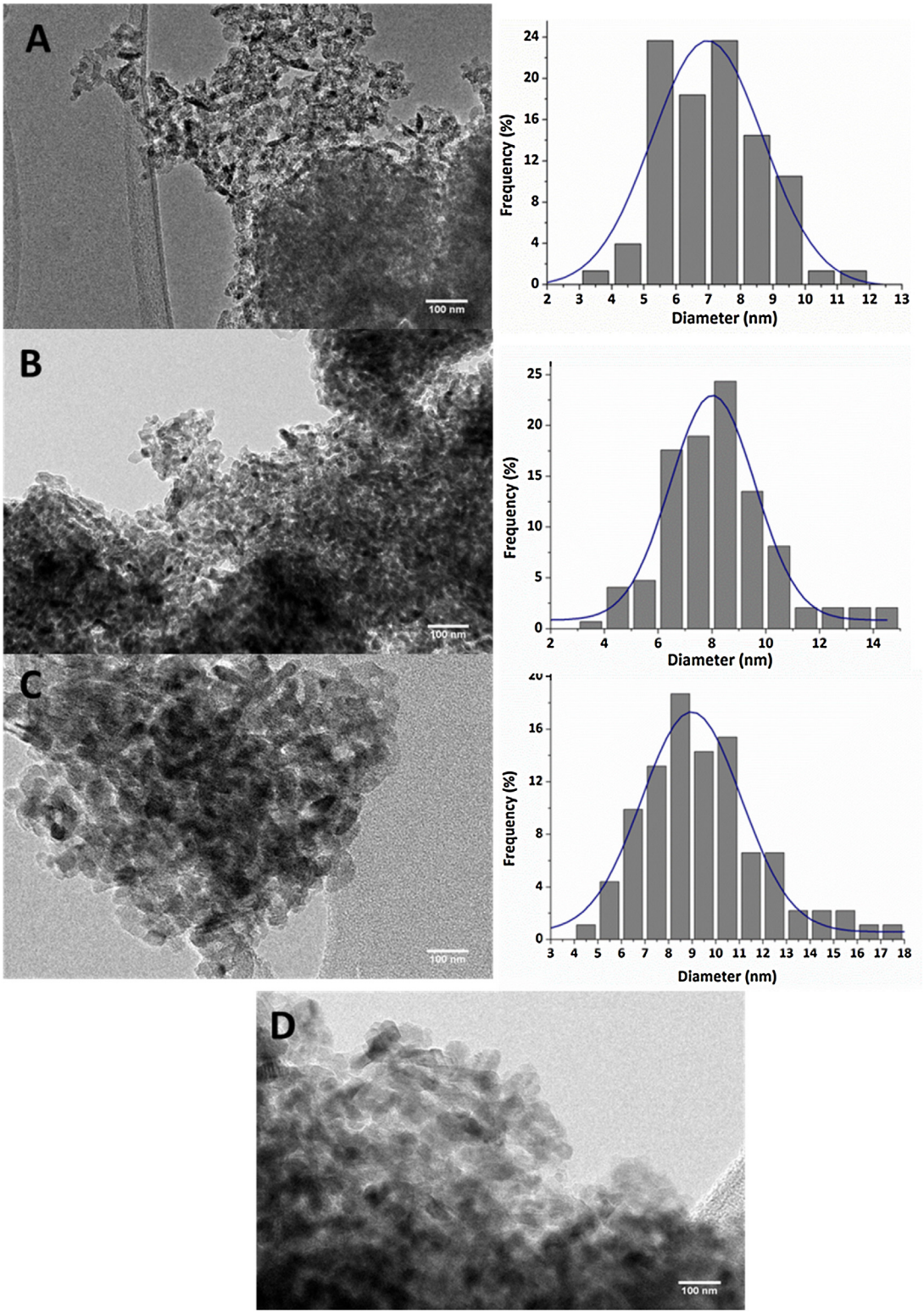

Fig. 3. HR-TEM micrographs of 5%Ni/TiO_2 (A), 10%Ni/TiO_2 (B), 15%Ni/TiO_2 (C) and (D) pure TiO_2 (anatase) substrate.

For oxygen atoms two contributions are observed, the O1s component at lower energy (529.9 eV) is due to Ti—O bond type of the TiO_2 network while higher energy component (531.5 eV) is associated with Ti—OH groups on the surface of the support [42,43]. The Ti $2p_{3/2}$ peak centered at 458.6 eV is associated to the presence of Ti^{4+} species in the catalyst. As expected, an increase in the Ni loading led to an increase of the surface exposure of Ni species (Table 4). Because of the decrease of metal-support interaction with an increase of Ni content, the percentage of Ni^0 species (given in parenthesis in Table 4) increases also confirming easier Ni reduction for the sample with largest Ni content. Moreover, XPS analysis indicates the absence of SMSI effect, because contributions from the binding energy are not shifted to smaller values of energy, which should be observed if reducible

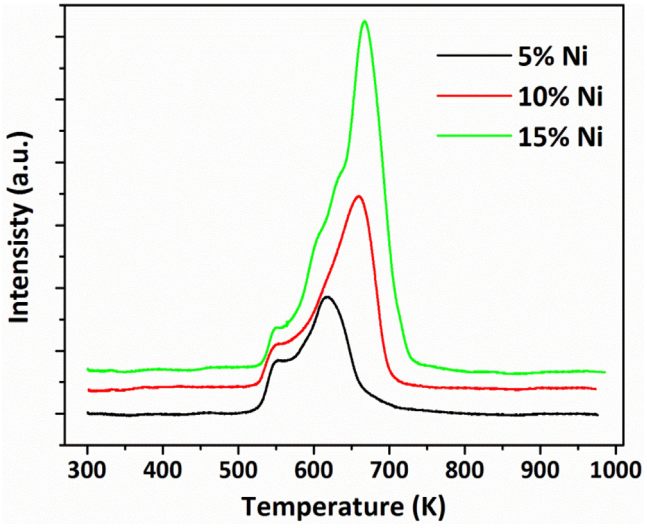

Fig. 4. H_2-TPR profiles of calcined x%Ni/TiO_2 samples (x = 5, 10, and 15 wt.% of Ni).

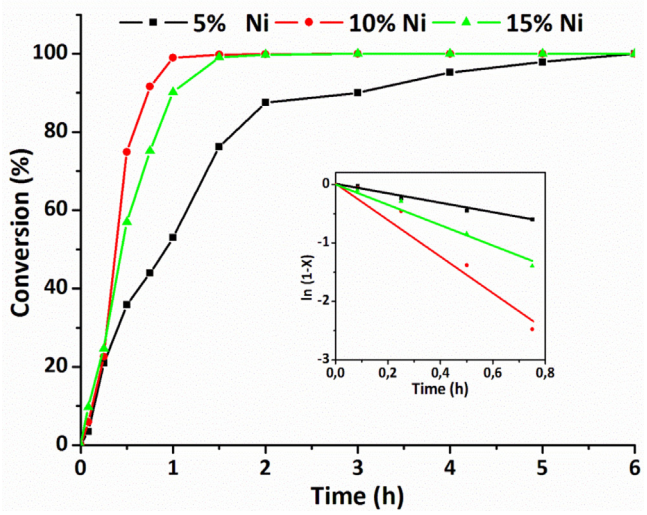

Fig. 5. Influence of Ni loading on maleic anhydride transformations on reduced x%Ni/TiO_2 catalysts. Reaction conditions: substrate/metal = 100, P_{H2}: 4.0 MPa; catalyst mass: 0.100 g; stirring rate: 650 rpm; solvent: THF; T = 373 K; reaction time of 6 h. The plot ln(1-X) vs. time (h) is shown in inlet of this figure.

species exist on the catalyst surface, indicating the absence of electronic enrichment in the metal particle due to TiO_x species [44].

3.2. Catalytic activity

3.2.1. Maleic anhydride hydrogenation

It is known that the production of succinic anhydride by catalytic hydrogenation of MA can be accompanied by a series of successive reactions (see Scheme 1), depending on the operating conditions and the nature of the catalyst. Another operational disadvantage is the high reactivity of the substrate (MA) against nucleophilic species (protic by-products, water, among others). Due to these features the catalytic reactions were carried out under anhydrous conditions. Careful drying of the solvent was performed, and the catalytic system was gassed until reach the reaction temperature, and thereafter the system was pressurized with H_2.

Influence of Ni loading on maleic anhydride transformations over reduced x%Ni/TiO_2 catalysts is shown in Fig. 5. All systems exhibit high activity in the target reaction: the two 10%Ni/TiO_2 and 15%Ni/TiO_2 catalysts exhibit a 100% of MA conversion at 2 h reaction whereas total MA conversion for 5%Ni/TiO_2 sample occur at 6 h of reaction time. Taking into account the literature information [45,46], the catalysts with Ni loading lower than 5 wt.% should be less effective in the target reaction. This is probably because the intrinsic hydrogenation property of Ni is much lower when compared with noble metals. This fact is commonly compensated by employing a much larger amount of Ni than in case of noble metals [47]. The effect of Ni loading (in range 3–30 wt.% of Ni) on the activity and selectivity of the Ni/HY-Al_2O_3 catalysts in hydrogenation of maleic anhydride to succinic anhydride was systematically investigated by Li et al. [45]. As expected, it was found that catalyst loaded with 3 wt.% of Ni exhibited lower activity and selectivity than that loaded with 5 wt.% of Ni being the latter the most optimized one [45,46]. Thus, we assume that our 5Ni/TiO_2 catalyst is the optimized one.

Table 5
Catalytic data[a] for MA hydrogenation on reduced Ni/TiO_2 catalysts.

Catalyst	k[a] (h^{-1} g_{Ni}^{-1})
5%Ni/TiO_2	3.34
10%Ni/TiO_2	7.53
15%Ni/TiO_2	3.20

[a] Pseudo-first-order constant; reaction conditions: T = 373 K; P_{H2}: 4.0 MPa; substrate/metal ratio = 100; catalyst mass: 0.100 g; stirring rate: 650 rpm; solvent: THF; reaction time: 6 h.

All catalysts studied exhibit 100% of MA conversion at reaction time of 6 h. For high MA conversions (close to 100%), the hydrogenation of MA is generally assumed to be a first order reaction with respect to MA [48,49]. Indeed, the plots of the ln(1-X) versus time are straight lines indicating a first order reaction for the catalysts studied (see inlet in Fig. 5). Thus, the pseudo-first order reaction was chosen to estimate reaction rate constants (Table 5). The reaction rate constants follow the trend: 10%Ni/TiO_2 » 5%Ni/TiO_2 ≈ 15%Ni/TiO_2. Although at high conversions, the mass transfer of the aromatics could be important, the diffusional effect could be excluded because of the large pore diameter of all catalysts (9.7 nm–10.3 nm). In this sense, Toppinen et al. [50] observed that the liquid phase hydrogenation of benzene and alkylbenzenes over a commercial 16.6 wt.% Ni/Al_2O_3 catalyst was mainly dominated by intraparticle mass transfer resistance of hydrogen. The reactor dynamics itself was found to be much slower than the diffusion process inside the catalyst particle [50].

With regard to the selectivity, all catalysts displayed 100% selectivity to the SA formation, and other possible hydrogenation products were not detected. Thus, only the carbon-carbon double bond of maleic anhydride was hydrogenated upon moderate reaction conditions employed (T = 373 K; P_{H2}: 4.0 MPa). Interestingly, at higher reaction temperature than that used in this work (483 K vs. 373 K), the most active 5%Ni/HY-Al_2O_3 catalyst exhibited a lower yield of SA [45] than the 5%Ni/TiO_2 sample studied in this work (89.62 vs. 99%). Since all x%Ni/TiO_2 catalysts exhibited almost 100% selectivity toward succinic anhydride, it was impossible to conclude on the possible influence of SMSI on the selectivity toward this product.

Contrary to work by Li et al. [45], the selectivity toward SA did not decrease with an increase of Ni loading from 5 to 15 wt.% indicating that overhydrogenation of the SA to GBL in the MA hydrogenation over x%Ni/TiO_2 catalysts did not occur. This could be explained taking into account the absence of formation of TiO_x species after *in situ* reduction of the catalysts, as it was confirmed by XPS. This is because the presence of oxygen vacancies would interact directly with C=O group of maleic anhydride activating and favoring the production of GBL. In this sense, the enhance of activity of Ni/TiO_2 catalyst in hydrogenation of acetophenone was explained as due to: (i) the activation of the carbonyl group by oxygen bonding with Ti^{3+} cation or (ii) the creation of oxygen vacancy

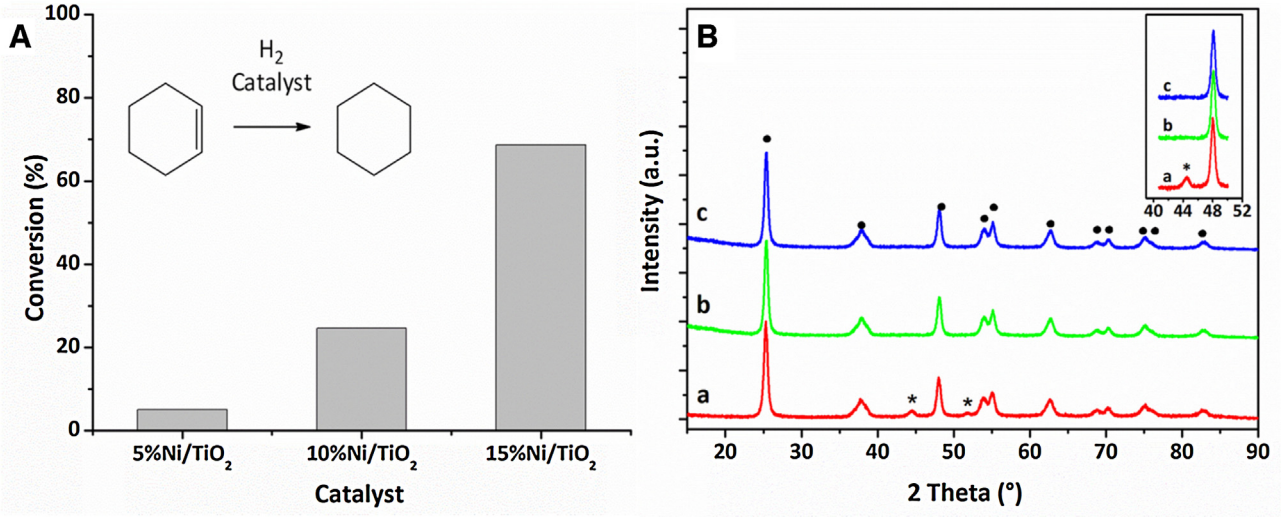

Fig. 6. (A) Influence of Ni loading on the cyclohexene conversion over *x*%Ni/TiO_2 catalysts (reaction conditions as in experimental section). (B) X-ray diffraction of the spent catalysts: (a) 5%Ni/TiO_2, (b) 10%Ni/TiO_2 and (b) 15%Ni/TiO_2. Reference patterns (*) Ni (JCPDS 00-004-0850), (●) TiO_2-Anatase (JCPDS 00-021-1272).

originated by SMSI effect [51]. Similarly, high selectivity toward crotyl alcohol was linked with the presence of partially reduced species, such as Pt—TiO_x and Ni—TiO_x, interacting with carbonyl group [37].

3.2.2. Leaching test and recycling

A major difficulty in using Ni catalysts is associated with their low operational stability in liquid phase reactions, mainly due to effects of leaching and agglomeration of the active phase by Ostwald effect [51]. Taking into account that the stability of Ni phase on the support surface during liquid phase operation strongly depends of the interaction of Ni species on the TiO_2 surface, the evaluation of Ni content before and after the activity test (Table 3) might give information on the influence of Ni loading on the Ni-TiO_2 interaction. Table 3 shows the ICP values for the catalysts after being subjected to the hydrogenation of MA. According to these results it can be assumed that an increase in the Ni coverage on the support surface decreases the stability of the active phase, increasing the metal leaching in the following order: 15%Ni/TiO_2 > 10%Ni/TiO_2 > 5%Ni/TiO_2. Thus, the 5%Ni/TiO_2 catalyst, despite having lower activity in the hydrogenation of MA, is the system that showed promising results in relation to its operational stability in the hydrogenation of MA, under the reaction conditions studied.

On the other hand, van Hassterecht et al. [52] have reported that catalyst deactivation may be due to two effects: (i) surface active phase oxidation and subsequent crowding; (ii) loss of Ni clusters from the surface of the catalysts to the solution, which can occur between successive cycles of the filtered steps. To confirm which of the two effects play a role in our systems, we have performed a study of the capacity of hydrogenation of the recovered filtrate after the hydrogenation of MA, results that are shown in Fig. 6A. For this study cyclohexene was chosen as substrate for the hydrogenation, in order to obtain an indirect measure of the leaching. Cyclohexene was used due to the high activity that this substrate has shown in hydrogenation reaction carried out by catalytic systems based on Ni nanoparticles [53].

For the three filtrates remains hydrogenating activity was observed, and the following order was obtained: 15%Ni/TiO_2 > 10%Ni/TiO_2 » 5%Ni/TiO_2. These results confirm that during the liquid phase reaction the systems with loading greater than 5% Ni present an important loss of active phase. XRD post-reaction characterization of the three catalysts can be observed in Fig. 6B. Systems 10%Ni/TiO_2 and 15%Ni/TiO_2 show predominant

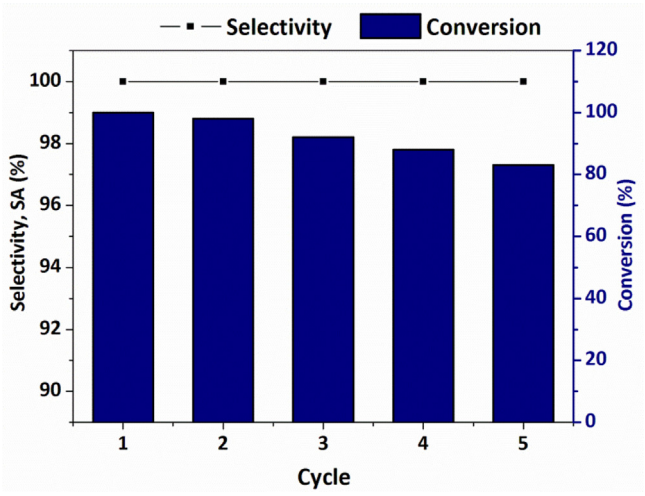

Fig. 7. Conversion level and selectivity in function of the number of reaction cycles for the catalyst 5% Ni/TiO_2. Reaction conditions: substrate/metal = 100; P_{H2}: 40 bar; catalyst mass: 0.100 g; stirring rate: 650 rpm; solvent: THF; *T* = 373 K; reaction time: 6 h.

diffraction lines associated to the support, along with the disappearance of diffraction lines attributed to Ni^0. For the 5%Ni/TiO_2 system no significant changes between the fresh catalyst and the used one were observed. With these results it can be assumed that the deactivation of the catalyst is mainly due to leaching of Ni^0 and not to the agglomeration of oxide particles on the surface, since XRD analysis did not show diffraction peaks associated to Ni_xO_y species.

Since the 5%Ni/TiO_2 catalyst showed the best operational stability, five consecutive reaction cycles were performed for this system, and the results of the activity and selectivity for the different reaction cycles are shown in Fig. 7. In all cycles a 100% of selectivity towards SA was achieved, with a slight decrease of the activity along of catalytic cycles. This lowering in the catalytic activity can be attributed to slight leaching of Ni, as deduced from ICP-AES characterization of the spent catalysts (see Table 3)

3.2.3. Temperature effect

The effect of the reaction temperature (323 K–398 K) on the catalyst activity and selectivity in the MA hydrogenation toward SA was investigated also. The 5%Ni/TiO_2 catalyst was selected to this study because this sample showed the best operational stability in the target reaction at 373 K. In good agreement with literature [54],

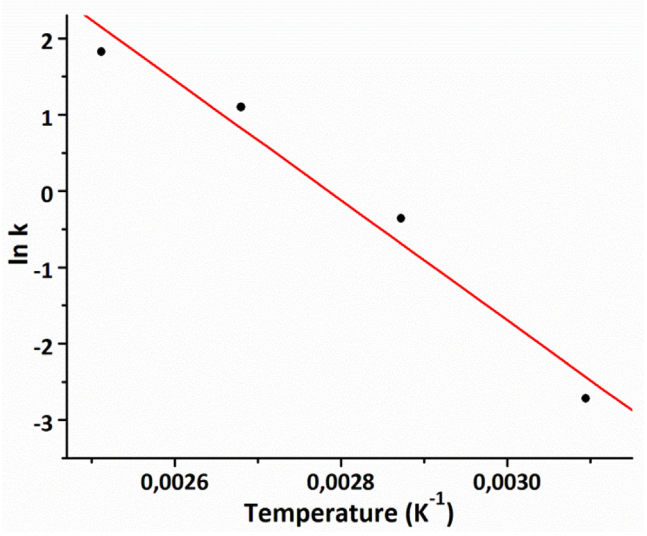

Fig. 8. Arrhenius plot for the hydrogenation of maleic anhydride on 5%Ni/TiO_2 catalyst. Reaction conditions: substrate/metal = 100, P_{H2}: 4.0 MPa; catalyst mass: 0.100 g; stirring rate: 650 rpm; solvent: THF; reaction time: 6 h.

an increase of activity with increasing temperature from 323 K to 398 K was observed. An Arrhenius plot showing ln*k* versus reaction temperature is shown in Fig. 8. As seen, the pseudo-first reaction rate constants fell on the straight line. The apparent activation energy (E_a), calculated from the slope of the Arrhenius plot straight line, was found to be 61.7 kJ mol^{-1}. Concerning the selectivity, the general observation is that the selectivity in the MA hydrogenation reaction depends on the reaction temperature [12,17]. However, in the range of temperatures studied (323 K–398 K), the 5%Ni/TiO_2 catalyst exhibit 100% of selectivity toward succinic anhydride.

4. Conclusions

Ni/TiO_2 catalysts prepared by wet impregnation with different metal contents, was found to be highly active and selective (100%) in the production of succinic anhydride by the hydrogenation of maleic anhydride at low reaction temperature (323 K–398 K). The textural characterization of the catalysts showed that the increase in Ni coverage on the surface of TiO_2 increases the size distribution of metallic particles. All systems showed incomplete reduction of the active phase on the reduction conditions employed, observing Ni_xO_y type species as revealed by the XPS analysis of the catalysts. At a reaction temperature of 373 K the data showed an activity dependence on the size of crystal. The characterization of spent catalysts demonstrated a strong dependence of catalyst stability on the nickel loading due to leaching of the active phase during the catalytic reaction. As a consequence, the catalyst stability during time curse of reaction presented the following trend: 5%NiTiO_2 > 10%Ni/TiO_2 > 15%Ni/TiO_2. Finally, the 5%Ni/TiO_2 catalyst was active and 100% selective to the production of succinic anhydride during five consecutive cycles without significant loss of activity.

Acknowledgements

The authors thank FONDECYT postdoctoral grant 3140157. C. Mella thanks CONICYT for doctoral fellowship 21150195. B. Pawelec expresses her gratitude to Comunidad de Madrid (Project CAM S2013/MAE-2882) for their financial support.

References

[1] K. Wilson, A.F. Lee, Philos. Trans. R. Soc. A: Math. Phys. Eng. Sci. 374 (2016).
[2] M.J. Climent, A. Corma, S. Iborra, L. Marti, ChemCatChem 8 (2016) 1335–1345.
[3] A. Küksal, E. Klemm, G. Emig, Appl. Catal. A: Gen. 228 (2002) 237–251.
[4] J. Kanetaka, T. Asano, S. Masamune, Ind. Eng. Chem. 62 (1970) 24–32.
[5] S.M. Jung, E. Godard, S.Y. Jung, K.-C. Park, J.U. Choi, J. Mol. Catal. A: Chem. 198 (2003) 297–302.
[6] U.R. Pillai, E. Sahle-Demessie, Chem. Commun. (2002) 422–423.
[7] G.L. Castiglioni, M. Ferrari, A. Guercio, A. Vaccari, R. Lancia, C. Fumagalli, Catal. Today 27 (1996) 181–186.
[8] Y. Feng, H. Yin, A. Wang, T. Xie, T. Jiang, Appl. Catal. A 425–426 (2012) 205–212.
[9] W. Yang, Z. Chen, X. Jiang, Y. Hu, Y. Li, Y. Shi, J. Wang, J. Mol. Liq. 180 (2013) 7–11.
[10] U.G. Hong, S. Hwang, J.G. Seo, J. Lee, I.K. Song, J. Ind. Eng. Chem. 17 (2011) 316–320.
[11] Y. Huang, Y. Ma, Y. Cheng, L. Wang, X. Li, Appl. Catal. A 495 (2015) 124–130.
[12] H. Jeong, T. Hwan Kim, K. Ill Kim, S. Haeng Cho, Fuel Process. Technol. 87 (2006) 497–503.
[13] X. Liao, Y. Zhang, M. Hill, X. Xia, Y. Zhao, Z. Jiang, Appl. Catal. A 488 (2014) 256–264.
[14] A. Wang, H. Yin, H. Lu, J. Xue, M. Ren, T. Jiang, Catal. Commun. 10 (2009) 2060–2064.
[15] M.V. Rajashekharam, I. Bergault, P. Fouilloux, D. Schweich, H. Delmas, R.V. Chaudhari, Catal. Today 48 (1999) 83–92.
[16] H. Zhao, H. Song, L. Chou, Inorg. Chem. Commun. 15 (2012) 261–265.
[17] Y.-L. Zhu, G.-W. Zhao, J. Chang, J. Yang, H.-Y. Zheng, H.-W. Xiang, Y.-W. Li, Catal. Lett. 96 (2004) 123–127.
[18] W. Huo, C. Zhang, H. Yuan, M. Jia, C. Ning, Y. Tang, Y. Zhang, J. Luo, Z. Wang, W. Zhang, J. Ind. Eng. Chem. 20 (2014) 4140–4145.
[19] S. Bagheri, N. Muhd Julkapli, S. Bee Abd Hamid, J. Sci. World 2014 (2014) 21.
[20] Y. Liang, H. Zhang, H. Zhong, X. Zhu, Z. Tian, D. Xu, B. Yi, J. Catal. 238 (2006) 468–476.
[21] W. Yan, S.M. Mahurin, Z. Pan, S.H. Overbury, S. Dai, J. Am. Chem. Soc. 127 (2005) 10480–10481.
[22] X. Ren, H. Zhang, Z. Cui, Mater. Res. Bull. 42 (2007) 2202–2210.
[23] N. Marín-Astorga, G. Pecchi, J.L.G. Fierro, P. Reyes, J. Mol. Catal. A: Chem. 231 (2005) 67–74.
[24] K. Joseph Antony Raj, M.G. Prakash, R. Mahalakshmy, T. Elangovan, B. Viswanathan, J. Mol. Catal. A: Chem. 366 (2013) 92–98.
[25] K.J.A. Raj, M.G. Prakash, R. Mahalakshmy, T. Elangovan, B. Viswanathan, Chin. J. Catal. 33 (2012) 1299–1305.
[26] E.P. Barrett, L.G. Joyner, P.P. Halenda, J. Am. Chem. Soc. 73 (1951) 373–380.
[27] M. Boudart, Adv. Catal. 20 (1969) 153–166.
[28] C.H. Campos, M. Jofré, C.C. Torres, B. Pawelec, J.L.G. Fierro, P. Reyes, Appl. Catal. A 482 (2014) 127–136.
[29] C.C. Torres, J.B. Alderete, G. Pecchi, C.H. Campos, P. Reyes, B. Pawelec, E.G. Vaschetto, G.A. Eimer, Appl. Catal. A 517 (2016) 110–119.
[30] C.C. Torres, C.H. Campos, C. Díaz, V.A. Jiménez, F. Vidal, L. Guzmán, J.B. Alderete, Mater. Sci. Eng. C 65 (2016) 164–171.
[31] C. Torres, C. Campos, J.L.G. Fierro, M. Oportus, P. Reyes, Catal. Lett. 143 (2013) 763–771.
[32] X. Lin, L. Lin, K. Huang, X. Chen, W. Dai, X. Fu, Appl. Catal. B 168–169 (2015) 416–422.
[33] W. Lin, H. Cheng, J. Ming, Y. Yu, F. Zhao, J. Catal. 291 (2012) 149–154.
[34] E.T. Kho, J. Scott, R. Amal, Chem. Eng. Sci. 140 (2016) 161–170.
[35] V.G. Deshmane, S.L. Owen, R.Y. Abrokwah, D. Kuila, J. Mol. Catal. A: Chem. 408 (2015) 202–213.
[36] A. Martínez, G. Prieto, J. Rollán, J. Catal. 263 (2009) 292–305.
[37] A. Dandekar, M.A. Vannice, J. Catal. 183 (1999) 344–354.
[38] T. Wu, Q. Yan, H. Wan, J. Mol. Catal. A: Chem. 226 (2005) 41–48.
[39] W. Lin, H. Cheng, J. Ming, Y. Yu, F. Zhao, J. Catal. 291 (2012) 149–154.
[40] F. Pompeo, D. Gazzoli, N.N. Nichio, Int. J. Hydrogen Energy 34 (2009) 2260–2268.
[41] S. Li, Y. Xu, X. Wang, Y. Guo, Q. Mu, RSC Adv. 6 (2016) 28994–29002.
[42] I. Iatsunskyi, M. Kempiński, G. Nowaczyk, M. Jancelewicz, M. Pavlenko, K. Załęski, S. Jurga, Appl. Surf. Sci. 347 (2015) 777–783.
[43] N.B. Rahna, V. Kalarivalappil, M. Nageri, S.C. Pillai, S.J. Hinder, V. Kumar, B.K. Vijayan, Mater. Sci. Semicond. Process. 42 (2016) 303–310 (Part 3).
[44] J.C. Colmenares, A. Magdziarz, M.A. Aramendia, A. Marinas, J.M. Marinas, F.J. Urbano, J.A. Navio, Catal. Commun. 16 (2011) 1–6.
[45] J. Li, W.-P. Tian, L. Shi, Ind. Eng. Chem. Res. 49 (2010) 11837–11840.
[46] S. Guo, W. Tian, L. Shi, Transit. Metal Chem. 37 (2012) 757–763.
[47] D.K. Cromwell, P.T. Vasudevan, B. Pawelec, J.L.G. Fierro, Catal. Today 259 (2016) 119–129 (Part 1).
[48] U. Herrmann, G. Emig, Chem. Eng. Technol. 21 (1998) 285–295.
[49] J. Kanetaka, S. Kiryu, T. Asano, S. Masamune, Bull. Jpn. Pet. Inst. 12 (1970) 89–96.
[50] S. Toppinen, T.-K. Rantakylä, T. Salml, J. Aittamaa, Catal. Today 38 (1997) 23–30.
[51] P.S. Kumbhar, Appl. Catal. A 96 (1993) 241–252.
[52] T. van Haasterecht, C.C.I. Ludding, K.P. de Jong, J.H. Bitter, J. Catal. 319 (2014) 27–35 (9).
[53] P. Migowski, G. Machado, S.R. Texeira, M.C.M. Alves, J. Morais, A. Traverse, J. Dupont, Phys. Chem. Chem. Phys. 9 (2007) 4814–4821.
[54] J. Li, W.-P. Tian, L. Shi, Catal. Lett. 141 (2011) 565–571.